Observed emergence of the climate change signal: from the familiar to the unknown

E. Hawkins[1], D. Frame[2], L. Harrington[3], M. Joshi[4], A. King[5], M. Rojas[6], and R. Sutton[1]

[1] National Centre for Atmospheric Science, Department of Meteorology, University of Reading.

[2] New Zealand Climate Change Research Institute, Victoria University of Wellington, Wellington 6012, New Zealand.

[3]

[4] Climatic Research Unit, School of Environmental Sciences, University of East Anglia, UK

[5] School of Earth Sciences and ARC Centre of Excellence for Climate Extremes, University of Melbourne.

[6] Department of Geophysics and Centre for Climate and Resilience Research, CR2, University of Chile

Corresponding author: Ed Hawkins (e.hawkins@reading.ac.uk)

Key Points:

- The signal of changes in observed temperature and rainfall due to global warming has clearly emerged in many regions and at meso-scales
- Tropical regions have experienced the largest changes in temperature relative to the amplitude of internal variability
- Signals of increasing extreme rainfall are emerging more quickly than signals in mean rainfall over many parts of the UK

Abstract

Changes in climate are usually considered in terms of trends or differences over time. However, for many impacts requiring adaptation, it is the amplitude of the change relative to the local amplitude of climate variability which is more relevant. Here, we explore the concept of 'signal-to-noise' in observations of local temperature, highlighting that many regions are already experiencing a climate which would be 'unknown' by late 19th century standards. The emergence of temperature changes over both land and ocean is clearest in tropical regions, in contrast to the regions of largest change which are in the northern extra-tropics – broadly consistent with climate model simulations. Significant increases and decreases in rainfall have also already emerged in different regions with the UK experiencing a shift towards more extreme rainfall events, a signal which is emerging more clearly in some places than the changes in mean rainfall.

Plain Language Summary

Changes in climate are translated into impacts on society not just though the amount of change, but how this change compares to the variations in climate that society is used to. Here we demonstrate that significant changes, when compared to the size of past variations, are present in both temperature and rainfall observations over many parts of the world.

1 Introduction

It was first noted that surface air temperatures were increasing at both local and global scales more than 80 years ago [*Kincer* 1933, *Callendar* 1938]. At the time it was unclear whether the observed changes were part of a longer term trend or a natural fluctuation – the 'signal' had not yet clearly emerged from the 'noise' of variability – although *Callendar* [1938] did suggest that the increase in atmospheric carbon dioxide concentrations was partly to blame.

The concept of the emergence of a climate change signal has since been discussed extensively, often linked with the detection & attribution of climatic changes. For example, *Madden & Ramanathan* [1980] and *Wigley & Jones* [1981] could not robustly detect the carbon dioxide warming signal, but *Hansen et al.* [1988] predicted that the ratio of temperature change and the magnitude of interannual variability – the signal-to-noise ratio – would be above 3 in large parts of the tropics by the 2010s, with smaller values over high latitude land regions. *Mahlstein et al.* [2011, 2012] subsequently demonstrated that the signal had indeed emerged in the observations, especially in the tropics in boreal summer, and with a similar pattern to that expected from climate model simulations. *Lehner et al.* [2017] subsequently highlighted emergence of observed temperature changes in both winter and summer in the northern extra-tropics. Significant changes in precipitation are often harder to detect because both thermodynamic and dynamic factors are crucial [e.g. *Zappa & Shepherd*, 2017] and because internal variability in precipitation is larger. However, precipitation changes are apparent in some regions [e.g. *Zhang et al.* 2007] including in extremes [e.g. *Min et al.* 2011].

Many studies have also considered when further changes in climate will emerge, for both mean temperature [*Mahlstein et al.* 2011, *Hawkins & Sutton* 2012] and precipitation [*Giorgi & Bi* 2009, *Fischer et al.* 2014]. Other studies have considered when changes in climate extremes should have emerged in the past [*King et al.* 2015] or future [*Diffenbaugh & Scherer* 2011,

Fischer et al. 2014]. However, rather than examine the timing of any climate emergence, we focus here on the related quantity – signal-to-noise.

The clearest emergence of warming – and largest signal-to-noise values – tend to be found in the tropics, which are regions with large and vulnerable populations [*Frame et al.* 2017, *Harrington et al.* 2017]. Signal-to-noise (S/N) is important for climate impacts, especially for ecosystems which have a limited ability to adapt and so large changes outside past experience could be particularly harmful [*Deutsch et al.* 2008; *Beaumont et al.* 2011]. Crop growing areas also face unprecedented heat [*Battisti & Naylor* 2009] and changes in rainfall which may move outside past experiences [*Rojas et al.* 2019]. The impacts of shifts in snowfall [*Diffenbaugh et al.* 2012] and Köppen–Geiger zones [*Mahlstein et al.* 2013] have also been discussed in terms related to the natural variability of the local conditions. Quantifying the changes that have already occurred may help determine which regions are suffering the largest adverse consequences of a warming world.

Here, we revisit the question of where and how the signal of climatic changes is emerging from the background noise of internal variability. In contrast to most previous studies we focus our analysis on observational datasets of temperature and precipitation, with model simulations used only to test the methodology.

2. Observed emergence and signal-to-noise

2.1 Methodology

Our aim is to produce estimates of signal-to-noise (S/N) for changes in observed climate variables without utilising data from any climate model simulations. The simple approach adopted is to linearly regress local variations in climate onto annual global mean surface temperature change (GMST), i.e.

$$L(t) = \alpha G(t) + \beta,$$

where $L(t)$ is the local change (in temperature or precipitation) over time, $G(t)$ is a smoothed version of GMST change over the same period, α defines the linear scaling between L and G, and β is a constant. *Sutton et al.* [2015] highlighted that a large fraction of variance in local climate changes can be represented by GMST changes, and *Fischer et al.* [2014] demonstrated that a similar regression approach provided robust estimates of S/N when examining future changes in precipitation in climate model simulations.

For $G(t)$ we use GMST from the Berkeley Earth temperature dataset for 1850-2018 (*Rohde et al.* [2013], combined with HadSST3 from *Kennedy et al.* [2011]), relative to the mean of 1850-1900, and smoothed with a lowess filter of 41-years to highlight the long-term variations (Figure 1a). The conclusions are insensitive to whether the smoothing parameter is slightly larger or smaller. The ‘signal’ of global temperature change is defined as the value of the smoothed

GMST in 2018 (G_{2018} = 1.19K), the 'signal' of local climate change explained by GMST is αG and the 'noise' is defined as the standard deviation of the residuals ($L - \alpha G$).

Although we do not formally attribute the observed change in GMST, and hence local changes, to particular radiative forcings or feedbacks, applying the method of *Haustein et al.* [2017] to derive a GMST change that is attributable to human activity gives 1.22K, similar to G_{2018}. Although 1850-1900 is often considered as a proxy for 'pre-industrial' GMST, the *Haustein et al.* [2017] approach also suggests an additional anthropogenic warming of around 0.05K occurred between 1750 and 1850-1900, based on radiative forcing estimates back to 1750. Although this plausible pre-1850 attributable warming is not included in our analysis, we refer to the 1850-1900 period as the early-industrial era, rather than pre-industrial.

2.2 Example for annual mean temperatures in Oxford

To demonstrate our approach we consider a case study of temperature change in Oxford, UK. *Burt & Burt* [2019] produced an extended temperature record for the Oxford Radcliffe Observatory with annual means available for 1814-2018. The temporal evolution of GMST and temperatures in Oxford are similar, showing that the 'fingerprint' of GMST change is clearly visible at the spatial scale of a single continuous weather station, although with more noise at the local scale (Figure 1b, also see *Sutton et al.* [2015]). We note that there is likely an urban heat island influence on temperatures in Oxford of around 0.1-0.2K [*Burt & Burt* 2019].

We regress this local temperature dataset onto smoothed GMST and obtain $\alpha = 1.45 \pm 0.25$ (95% confidence interval). The 'signal' for Oxford is $\alpha G_{2018} = 1.72 \pm 0.30$K and the 'noise', i.e. the local variations that are not explained by GMST variations, is 0.54K. Oxford therefore exhibits a S/N ratio of 3.2 ± 0.5 (Figure 1b).

We adopt the language of *Frame et al.* [2017] to describe how the climate has changed from being familiar, to being '*unusual*' relative to lived experience (S/N > 2), '*unknown*' (S/N > 3), and here we introduce '*inconceivable*' for S/N values above 5 (Fig. S1). Using this terminology, temperatures in Oxford have become unknown relative to the early-industrial era. Two other regional examples are illustrated in Fig. S2.

2.3 Local climate data and methodological tests

We perform a similar S/N analysis for each land and ocean gridpoint in the Berkeley Earth temperature dataset (1850-2018) and in the GPCCv2018 land precipitation dataset (1891-2016, *Schneider et al.* [2017]). We use the 1º x 1º datasets for both Berkeley Earth and GPCC. We also use the HadUK-Grid dataset for the UK [*Hollis et al.* 2019] at 25km spatial resolution for monthly (1862-2017) and daily (1891-2017) precipitation data to examine changes in mean rainfall and extremes. Note that smoothed GMST (1850-2018) is used as G for both local temperature and precipitation analyses.

As the local data is not necessarily available for all years back to 1850 we perform the regression only over the period where local temperatures or precipitation are defined. The signal relative to the early-industrial era can still be calculated assuming that the estimated regression parameter (α), is representative for the whole period, i.e. the signal is always αG_{2018}, irrespective of the

time period used to calculate α. However, we require that there must be at least 100 years of local climate data available.

We test our methodology using a large ensemble of climate simulations for the historical period [*Maher et al.* 2019], specifically to examine the uncertainty due to internal variability in derived S/N values for temperature and precipitation. Figs. S3 and S4 demonstrate that the methodology produces S/N values with small uncertainties (typically <0.4 over land regions) and robust patterns.

3. Emergence of unknown temperatures

The map of the current observed signal of annual temperature change, relative to the early-industrial era, is shown in Figure 2a. It shows the familiar pattern of more warming over land than over the oceans, more warming at high northern latitudes, and less warming in the tropical regions and the southern hemisphere. Virtually all locations have experienced more than 1K change since the early-industrial era, and many regions have exceeded 2K. The estimated noise shows a similar pattern with larger variability at higher northern latitudes, but the differences between the tropics and extra-tropics are more pronounced than for the signal (Figure 2b).

The ratio of these two patterns results in a signal-to-noise (S/N) map with the largest values in the tropical regions (Figure 2c). Although these areas generally have smaller signals than higher latitude regions, they have experienced a larger amplitude change relative to the (smaller) background variations in temperature than other regions. This is important as societies, infrastructure and ecosystems are often adapted for the range of local climate experienced. S/N measures how far the climate is being shifted from that past range; the climate in large parts of the tropics has shifted such that the mean climate would have been inconceivable in the early-industrial era. More than half of the land area has experienced S/N above 3, and so has moved into a climate that is unknown by early-industrial standards (Fig. S5).

Over the oceans the largest S/N values are found in the tropical Atlantic and tropical Indian Oceans. Fish species such as tuna have already been seen to be moving away from the tropics to the sub-tropics, likely to avoid these warmer waters [*Monllor-Hurtado et al.* 2017]. Large parts of the North Atlantic have seen little warming overall, likely due to changes in ocean circulation providing a local cooling influence to offset global warming [e.g. *Dima & Lohmann* 2010].

Although there are variations in magnitude, the estimated S/N pattern is relatively robust to the choice of temperature dataset [*Morice et al.* 2012, *Cowtan & Way* 2014, *Lenssen et al.* 2019, *Zhang et al.* 2019]. However, there are notable local differences between datasets over south-east USA and parts of South America (Fig. S6). The overall observed emergence pattern is broadly similar to that found in models under future climate change scenarios [*Frame et al.*, 2017] though there are regional-scale differences; especially in the oceans but over some land areas too.

When considering how changes in climate may be experienced, it may in many cases be more relevant to examine seasonal or monthly timescales, depending on the impact being considered. For example, Figure 3 shows that S/N values can still be significant for monthly average temperatures. Again, the largest S/N values are found in the tropics and tend to be larger for the

climatologically warmest month than the climatologically coldest month for each location. This is because weather variability tends to be larger in the colder months. Around 40% of land areas have moved into an unusual climate in their warmest months, and 20% in the coldest months (Fig. S5). This suggests a comparatively large increase in likelihood of heat-related extreme events in already warm months of already hot countries. One example is south-east Asia where the S/N values are large and the combined effects of El Nino events and climate change on extreme heat in the warmest months of the year has previously been noted [*Thirumalai et al.* 2017].

4. Emergence of unusual precipitation amounts

The S/N analysis is repeated for annual mean precipitation using the GPCC dataset. In this case, some regions are getting significantly wetter and others are getting significantly drier (Figure 4) but, unsurprisingly, the signals are less clear than for temperature. Notable emergence of '*unfamiliar*' (S/N > 1) or unusual precipitation changes are observed in west Africa, Brazil, Chile and south-west Australia (drier), and the northern high latitudes and Argentina (wetter). The seasonal values of S/N are shown in Fig. S7. The changes in several of these regions have been discussed as being consistent with the expected response to increased greenhouse gas forcing, e.g. for south-west Australia [*Delworth & Zeng* 2014], for Chile [*Boisier et al.* 2016] and the northern extra-tropics [*Zhang et al.* 2007].

To demonstrate that this framework can be applied to a range of gridded datasets and spatial scales, we consider one small region in more detail. The UK has a gridded rainfall dataset available, covering 1891-2017 (daily) and 1862-2017 (monthly), which is suitable for examining changes in mean and extreme rainfall [*Hollis et al.* 2019].

Figure 5 shows the signal and S/N for annual mean rainfall, highlighting a tendency for increasing rainfall in large parts of the northern UK and the western coasts of up to 20% per K of GMST change. The corresponding S/N values exceed 1 in several areas, and these tend to be mountainous regions. Fig. S8 shows the seasonal mean S/N values.

When considering the wettest day of the year (RX1day) as $L(t)$, there is a clear signal of increasing extreme rainfall, but the pattern is strikingly different to the mean. This signal is visible across large parts of the UK, even in regions where there are only small changes in mean rainfall. The signal has only clearly emerged in a few locations (Fig. 5) but the spatial average of RX1day across the UK suggests an increase in extreme rainfall amounts of around 4mm (or 11%) per K of GMST change (Fig. S9), which is around 8% per K of UK temperature change, approximately consistent with Clausius-Clapeyron expectations [*Pall et al.* 2007].

These findings are consistent with *Min et al.* [2011] who showed that the signal of changes in extreme rainfall were detectable and attributable to human activity over large parts of the northern hemisphere land areas, and with *Fischer et al.* [2014] used climate model simulations to suggest that emergence of changes in extreme rainfall can occur earlier than changes in mean rainfall. Continued recovery of millions of undigitized weather observations, including for daily

rainfall, will improve and lengthen these gridded datasets [e.g. *Ashcroft et al.* 2018; *Hawkins et al.* 2019].

5. Summary and discussion

We have estimated the signal-to-noise ratio (S/N) of observed temperature and precipitation changes since the early-industrial era (1850-1900). Although we do not formally attribute these local changes to specific radiative forcings or feedbacks, the emergence of significantly different climates is related to increases in GMST, which itself is largely due to anthropogenic factors [e.g. *IPCC* 2018].

Consistent with previous studies and expectations from climate model simulations, the largest S/N values for historical temperature changes are seen in the tropical regions, over both land and ocean. Large regions have already experienced a shift to a climate state that is unknown, and even inconceivable, compared to that in the late 19th century. These signals of change are also clear in monthly average temperatures, with warmer months showing more significant changes.

Precipitation signals are emerging in several regions when considering observed rainfall changes, particularly West Africa, parts of South America and northern Eurasia. Some regions in South America and central Africa exhibit simultaneously high S/N for temperature ($S/N>4$) and significantly drier precipitation ($S/N<-1$) which may compound impacts.

As a demonstration of the methods in a data-rich region, and over a range of spatial scales, our analysis shows there are clear shifts towards more annual rainfall over the UK, focussed over northern and western areas. Significant increases in extreme heavy rainfall are emerging over large parts of the UK and are emerging more quickly than changes in mean rainfall in some places. The magnitude of the increase in extreme rainfall (~8% per K of local temperature change) is approximately consistent with expectations from the Clausius-Clapeyron relationship.

Many of the largest global shifts in climate, relative to the background variability, are found in countries with large, vulnerable populations, and this will be exacerbated if policy targets such as those in the Paris Agreement are not met [*Frame et al.* 2017, *King & Harrington* 2018]. There are also implications for ecosystems in these regions, which may not be able to adapt to such an unknown climate, especially given the rates of change. The rates of change of signal-to-noise to which societies and ecosystems can adapt is an important topic for future analyses.

Acknowledgments

EH and RS were supported by the National Centre for Atmospheric Science, and EH was funded by the INDECIS project. ADK was funded by the Australian Research Council (DE180100638). MJ is funded by UK Natural Environment Research Council grants NE/S004645/1 and NE/N018486/1. MR acknowledges funding from FONDAP-CONICYT 15110009.

References

Ashcroft, L., J. R. Coll, A. Gilabert, P. Domonkos, M. Brunet, E. Aguilar, M. Castella, J. Sigro, I. Harris, P. Unden and P. Jones, A rescued dataset of sub-daily meteorological

observations for Europe and the southern Mediterranean region, 1877–2012, Earth Syst. Sci. Data, 10, 1613–1635doi: 10.5194/essd-10-1613-2018, 2018

Battisti, D. S., and R. L. Naylor, Historical warnings of future food insecurity with unprecedented seasonal heat, Science, 323(5911), 240–244, doi:10. 1126/science.1164363, 2009.

Beaumont, L. J., A. Pitman, S. Perkins, N. E. Zimmermann, N. G. Yoccoz, and W. Thuiller, Impacts of climate change on the worlds most exceptional ecoregions, Proceedings of the National Academy of Sciences, 108 (6), 2306– 2311, doi:10.1073/pnas.1007217108, 2011.

Boisier, J. P., R. Rondanelli, R. D. Garreaud, and F. Munoz, Anthropogenic and natural contributions to the southeast pacific precipitation decline and recent megadrought in central Chile, Geophysical Research Letters, 43(1), 413–421, doi:10.1002/2015gl067265, 2016.

Burt, S. and Burt, T., Oxford Weather and Climate since 1767, Oxford University Press, 2019

Callendar, G. S., The artificial production of carbon dioxide and its influence on temperature, Quarterly Journal of the Royal Meteorological Society, 64(275), 223–240, doi:10.1002/qj.49706427503, 1938.

Cowtan, K., and R. G. Way, Coverage bias in the HadCRUT4 temperature series and its impact on recent temperature trends, Quarterly Journal of the Royal Meteorological Society, 140(683), 1935–1944, doi: 10.1002/qj.2297, 2014.

Delworth, T. L., and F. Zeng, Regional rainfall decline in Australia attributed to anthropogenic greenhouse gases and ozone levels, Nature Geoscience, 7(8), 583–587, doi:10.1038/ngeo2201, 2014.

Deutsch, C. A., J. J. Tewksbury, R. B. Huey, K. S. Sheldon, C. K. Ghalambor, D. C. Haak, and P. R. Martin, Impacts of climate warming on terrestrial ectotherms across latitude, Proceedings of the National Academy of Sciences, 105(18), 6668–6672, doi:10.1073/pnas.0709472105, 2008.

Diffenbaugh, N. S., and M. Scherer, Observational and model evidence of global emergence of permanent, unprecedented heat in the 20th and 21st centuries, Climatic Change, 107(3-4), 615–624, doi:10.1007/ s10584-011-0112-y, 2011.

Diffenbaugh, N. S., M. Scherer and M. Ashfaq, Response of snow-dependent hydrologic extremes to continued global warming, Nature Climate Change, 3, 379, doi: 10.1038/nclimate1732, 2013

Dima, M. and G. Lohmann, Evidence for Two Distinct Modes of Large-Scale Ocean Circulation Changes over the Last Century, Journal of Climate, 23, 5, doi: 10.1175/2009JCLI2867.1, 2010

Fischer, E. M., J. Sedlacek, E. Hawkins, and R. Knutti, Models agree on forced response pattern of precipitation and temperature extremes, Geophysical Research Letters, 41(23), 8554–8562, doi:10.1002/2014gl062018, 2014.

Frame, D., M. Joshi, E. Hawkins, L. J. Harrington, and M. de Roiste, Population-based emergence of unfamiliar climates, Nature Climate Change, 7(6), 407–411, doi:10.1038/nclimate3297, 2017.

Giorgi, F., and X. Bi, Time of emergence (TOE) of GHG-forced pre- cipitation change hot-spots, Geophysical Research Letters, 36(6), doi: 10.1029/2009gl037593, 2009.

Hansen, J., I. Fung, A. Lacis, D. Rind, S. Lebedeff, R. Ruedy, G. Russell, and P. Stone, Global climate changes as forecast by Goddard institute for space studies three-dimensional model, Journal of Geophysical Research, 93(D8), 9341, doi:10.1029/jd093id08p09341, 1988.

Harrington, L., D. Frame, E. Hawkins and M. Joshi, Seasonal cycles enhance disparities between low- and high-income countries in exposure to monthly temperature emergence with future warming, Environ. Res. Lett., 12, 114039, doi: 10.1088/1748-9326/aa95ae, 2017

Haustein, K., M. R. Allen, P. M. Forster, F. E. L. Otto, D. M. Mitchell, H. D. Matthews, and D. J. Frame, A real-time global warming index, Scientific Reports, 7(1), doi:10.1038/s41598-017-14828-5, 2017.

Hawkins, E., and R. Sutton, Time of emergence of climate signals, Geophysical Research Letters, 39 (1), doi:10.1029/2011gl050087, 2012.

Hawkins, E., S. Burt, P. Brohan, M. Lockwood, H. Richardson, M. Roy, and S. Thomas, Hourly weather observations from the Scottish highlands (1883–1904) rescued by volunteer citizen scientists, Geoscience Data Journal, doi:10.1002/gdj3.79, 2019.

Hollis, D., M. McCarthy, M. Kendon, T. Legg, and I. Simpson, HadUK-grid—a new UK dataset of gridded climate observations, Geoscience Data Journal, doi:10.1002/gdj3.78, 2019.

IPCC, Summary for Policymakers. In: Global Warming of 1.5°C. An IPCC Special Report on the impacts of global warming of 1.5°C above pre-industrial levels and related global greenhouse gas emission pathways, in the context of strengthening the global response to the threat of climate change, sustainable development, and efforts to eradicate poverty [Masson-Delmotte, V., P. Zhai, H.-O. Pörtner, D. Roberts, J. Skea, P.R. Shukla, A. Pirani, W. Moufouma-Okia, C. Péan, R. Pidcock, S. Connors, J.B.R. Matthews, Y. Chen, X. Zhou, M.I. Gomis, E. Lonnoy, T. Maycock, M. Tignor, and T. Waterfield (eds.)]. World Meteorological Organization, Geneva, Switzerland, 32 pp., 2018

Kennedy, J. J., N. A. Rayner, R. O. Smith, D. E. Parker, and M. Saunby, Reassessing biases and other uncertainties in sea surface temperature observations measured in situ since 1850: 1. measurement and sampling uncertainties, Journal of Geophysical Research, 116(D14), doi:10.1029/ 2010jd015218, 2011.

Kincer, J. B., Is our climate changing? A study of long-time temperature trends, Monthly Weather Review, 61 (9), 251– 259, doi:10.1175/1520-0493(1933)61⟨251:ioccas⟩2.0.co;2, 1933.

King, A. D., and L. J. Harrington, The inequality of climate change from 1.5 to 2c of global warming, Geophysical Research Letters, 45 (10), 5030–5033, doi:10.1029/2018gl078430, 2018.

King, A. D., M. G. Donat, E. M. Fischer, E. Hawkins, L. V. Alexander, D. J. Karoly, A. J. Dittus, S. C. Lewis, and S. E. Perkins, The timing of anthropogenic emergence in simulated climate extremes, Environmental Research Letters, 10(9), 094,015, doi:10.1088/1748-9326/10/9/094015, 2015.

Lehner, F., C. Deser, and L. Terray, Toward a new estimate of "time of emergence" of anthropogenic warming: Insights from dynamical adjustment and a large initial-condition model ensemble, Journal of Climate, 30(19), 7739–7756, doi:10.1175/jcli-d-16-0792.1, 2017.

Lenssen, N. J. L., G. A. Schmidt, J. E. Hansen, M. J. Menne, A. Persin, R. Ruedy, and D. Zyss, Improvements in the GISTEMP uncertainty model, Journal of Geophysical Research: Atmospheres, 124(12), 6307–6326, doi: 10.1029/2018jd029522, 2019.

Madden, R. A., and V. Ramanathan, Detecting climate change due to in- creasing carbon dioxide, Science, 209 (4458), 763–768, doi:10.1126/science. 209.4458.763, 1980.

Maher, N., et al., The Max Planck Institute grand ensemble: Enabling the exploration of climate system variability, Journal of Advances in Modeling Earth Systems, 11(7), 2050–2069, doi:10.1029/2019ms001639, 2019.

Mahlstein, I., R. Knutti, S. Solomon, and R. W. Portmann, Early onset of significant local warming in low latitude countries, Environmental Research Letters, 6(3), 034,009, doi:10.1088/1748-9326/6/3/034009, 2011.

Mahlstein, I., G. Hegerl, and S. Solomon, Emerging local warming signals in observational data, Geophysical Research Letters, 39 (21), doi: 10.1029/2012gl053952, 2012.

Mahlstein, I., J. S. Daniel, and S. Solomon, Pace of shifts in climate regions increases with global temperature, Nature Climate Change, 3, 739, doi: 10.1038/nclimate1876, 2013

Min, S.-K., X. Zhang, F. W. Zwiers, and G. C. Hegerl, Human contribution to more-intense precipitation extremes, Nature, 470(7334), 378–381, doi: 10.1038/nature09763, 2011.

Monllor-Hurtado, A., M. G. Pennino, and J. L. Sanchez-Lizaso, Shift in tuna catches due to ocean warming, PLOS ONE, 12(6), e0178,196, doi: 10.1371/journal.pone.0178196, 2017.

Morice, C. P., J. J. Kennedy, N. A. Rayner, and P. D. Jones, Quantifying uncertainties in global and regional temperature change using an ensemble of observational estimates: The HadCRUT4 data set, Journal of Geophysical Research: Atmospheres, 117(D8), n/a–n/a, doi:10.1029/2011jd017187, 2012.

Pall, P., M. R. Allen & D. A. Stone, Testing the Clausius–Clapeyron constraint on changes in extreme precipitation under CO_2 warming, Climate Dynamics, 28, 351, doi: 10.1007/s00382-006-0180-2, 2007

Rohde, R., R. A. Muller, R. Jacobsen, E. Muller, S. Perlmutter, A. Rosenfeld, J. Wurtele, D. Groom and C. Wickham, A New Estimate of the Average Earth Surface Land Temperature Spanning 1753 to 2011, Geoinfor Geostat, 1, 1, doi:10.4172/2327-4581.1000101, 2013

Rojas, M., F. Lambert, J. Ramirez-Villegas, and A. J. Challinor, Emergence of robust precipitation changes across crop production areas in the 21st century, Proceedings of the

National Academy of Sciences, 116 (14), 6673– 6678, doi:10.1073/pnas.1811463116, 2019.

Schneider, U., P. Finger, A. Meyer-Christoffer, E. Rustemeier, M. Ziese, and A. Becker, Evaluating the hydrological cycle over land using the newly- corrected precipitation climatology from the global precipitation climatology centre (GPCC), Atmosphere, 8(12), 52, doi:10.3390/atmos8030052, 2017.

Sutton, R., E. Suckling, and E. Hawkins, What does global mean tempera- ture tell us about local climate?, Philosophical Transactions of the Royal Society A: Mathematical, Physical and Engineering Sciences, 373(2054), 20140,426, doi:10.1098/rsta.2014.0426, 2015.

Thirumalai, K., P. N. DiNezio, Y. Okumura, and C. Deser, Extreme temperatures in southeast Asia caused by El Nino and worsened by global warming, Nature Communications, 8(1), doi:10.1038/ncomms15531, 2017.

Wigley, T. M. L. and P. D. Jones, Detecting CO_2-induced climatic change, *Nature*, 292, 205, 1981

Zappa, G. and T.G. Shepherd, Storylines of Atmospheric Circulation Change for European Regional Climate Impact Assessment. J. Climate, 30, 6561–6577, doi: 10.1175/JCLI-D-16-0807.1, 2017

Zhang, H.-M., et al., Updated temperature data give a sharper view of climate trends, Eos, 100, doi:10.1029/2019eo128229, 2019.

Zhang, X., F. W. Zwiers, G. C. Hegerl, F. H. Lambert, N. P. Gillett, S. Solomon, P. A. Stott, and T. Nozawa, Detection of human influence on twentieth-century precipitation trends, Nature, 448(7152), 461–465, doi: 10.1038/nature06025, 2007.

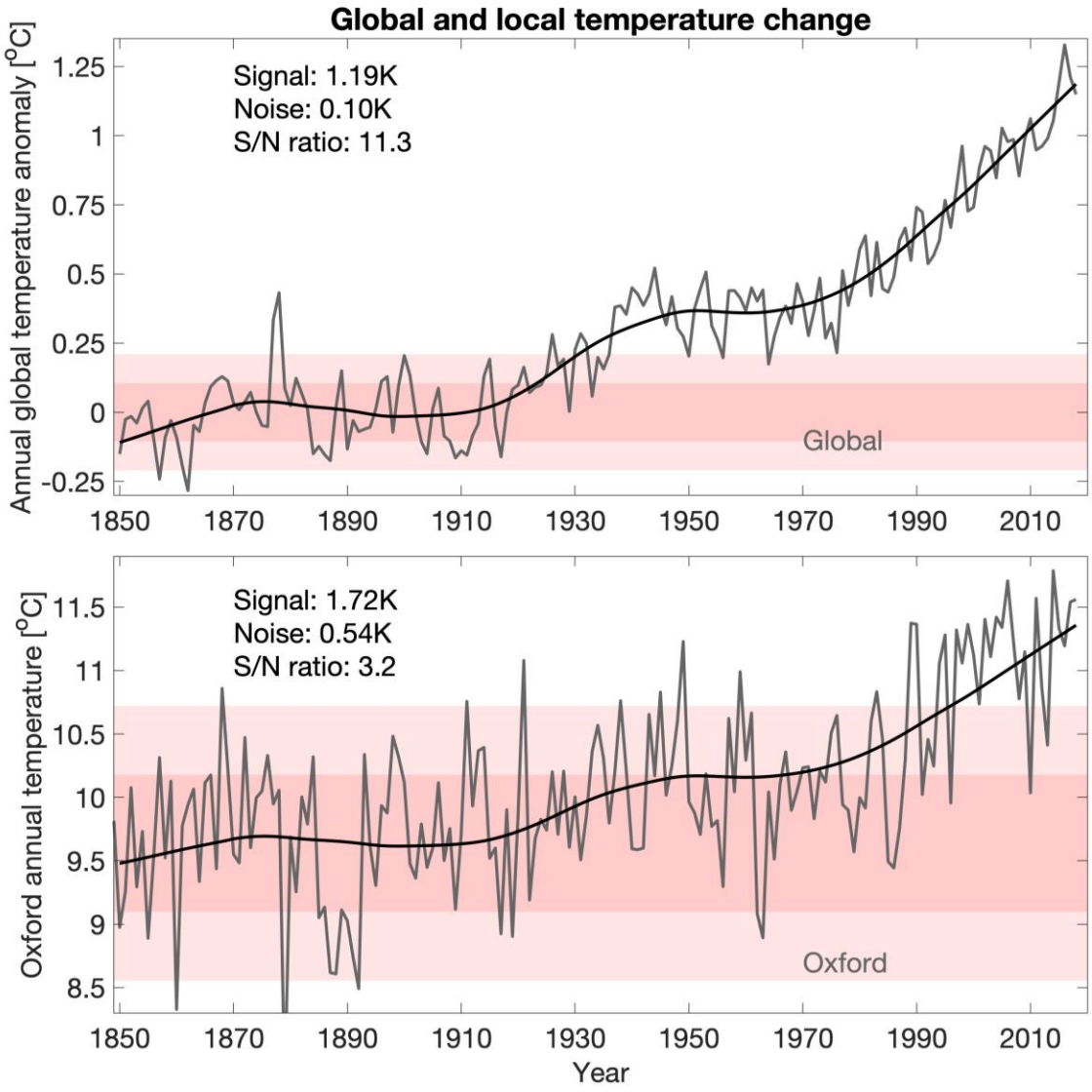

Figure 1: Emergence of global and local temperature change from 1850-2018. (top) GMST (grey), smoothed with a 41-year lowess filter (black). (bottom) Oxford annual temperature (grey) and scaled smoothed GMST (black). The correlation between Oxford temperatures and smoothed GMST is 0.67, and if the Oxford data is also smoothed with a 41-year lowess filter the correlation increases to 0.98. The shaded bands indicate 1 and 2 standard deviations of the noise.

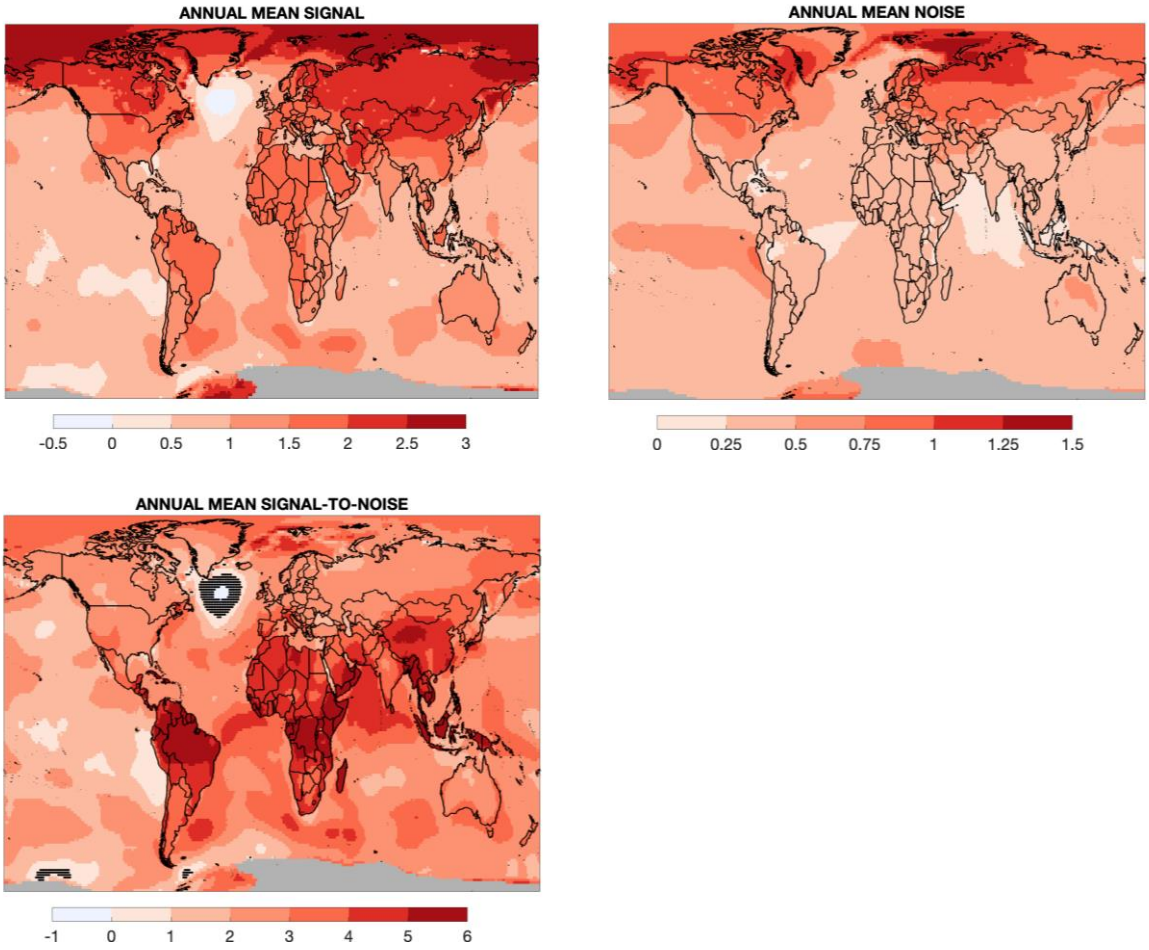

Figure 2: Signal, noise (both in K) and S/N for observed annual mean temperature change in the Berkeley Earth dataset. Many tropical regions show the smallest signal, but also the smallest noise and largest S/N. Grey regions denote lack of sufficient data. The S/N values in stippled areas are not significantly different from zero.

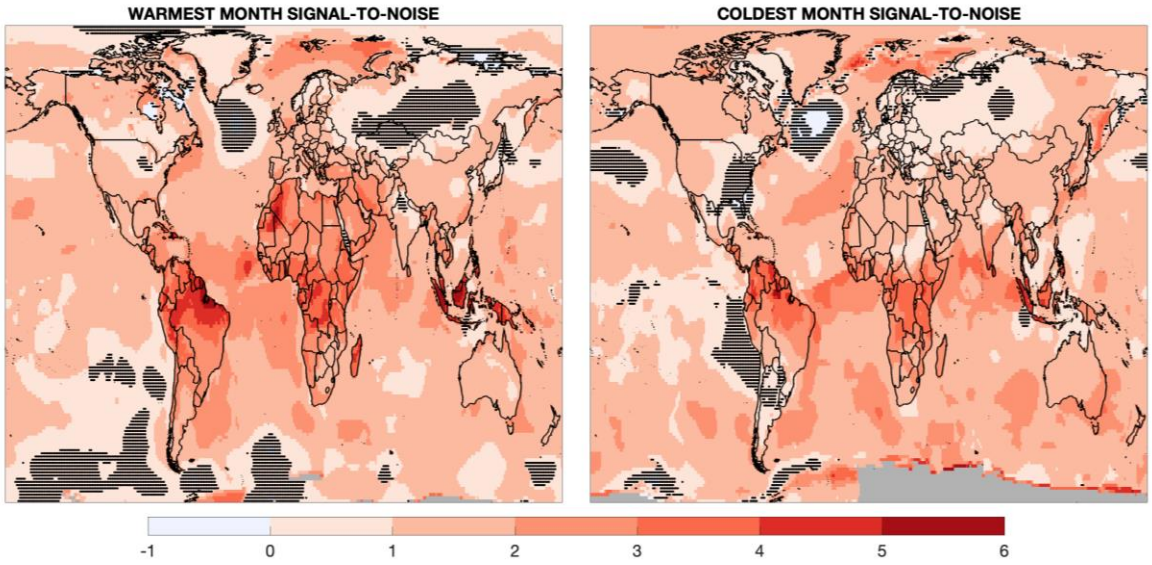

Figure 3: Signal-to-noise ratio for monthly average temperatures, for the climatologically warmest (left) and coldest (right) months at each grid point. Grey regions denote lack of sufficient data. The S/N values in stippled areas are not significantly different from zero.

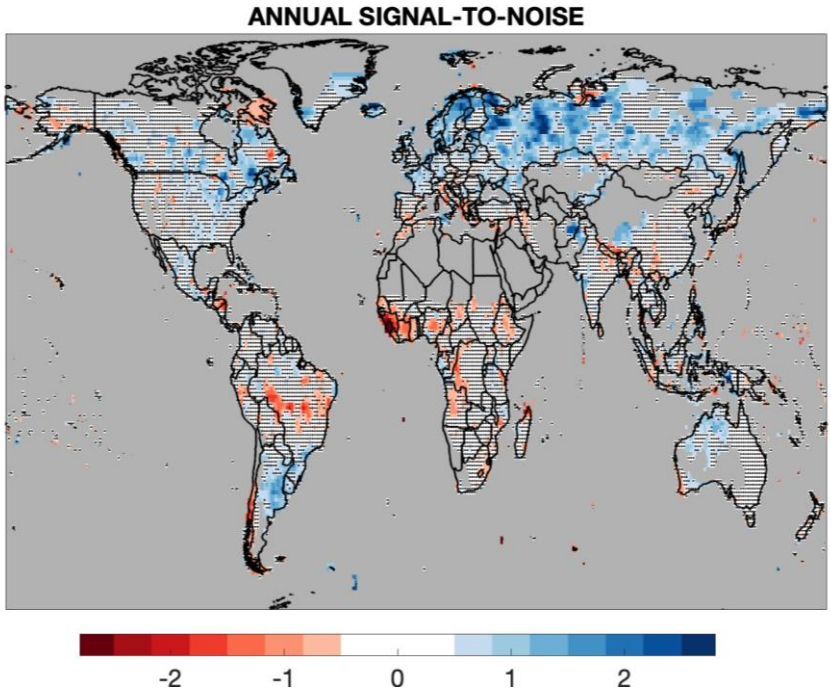

Figure 4: Signal-to-noise ratio for annual mean precipitation over land using the GPCC dataset. Blue colours denote regions becoming wetter, and red colours denote regions that are becoming drier. Grey regions are either unobserved (oceans) or deserts (<250mm/year). Stippling indicates where the regression parameter is not statistically significant from zero.

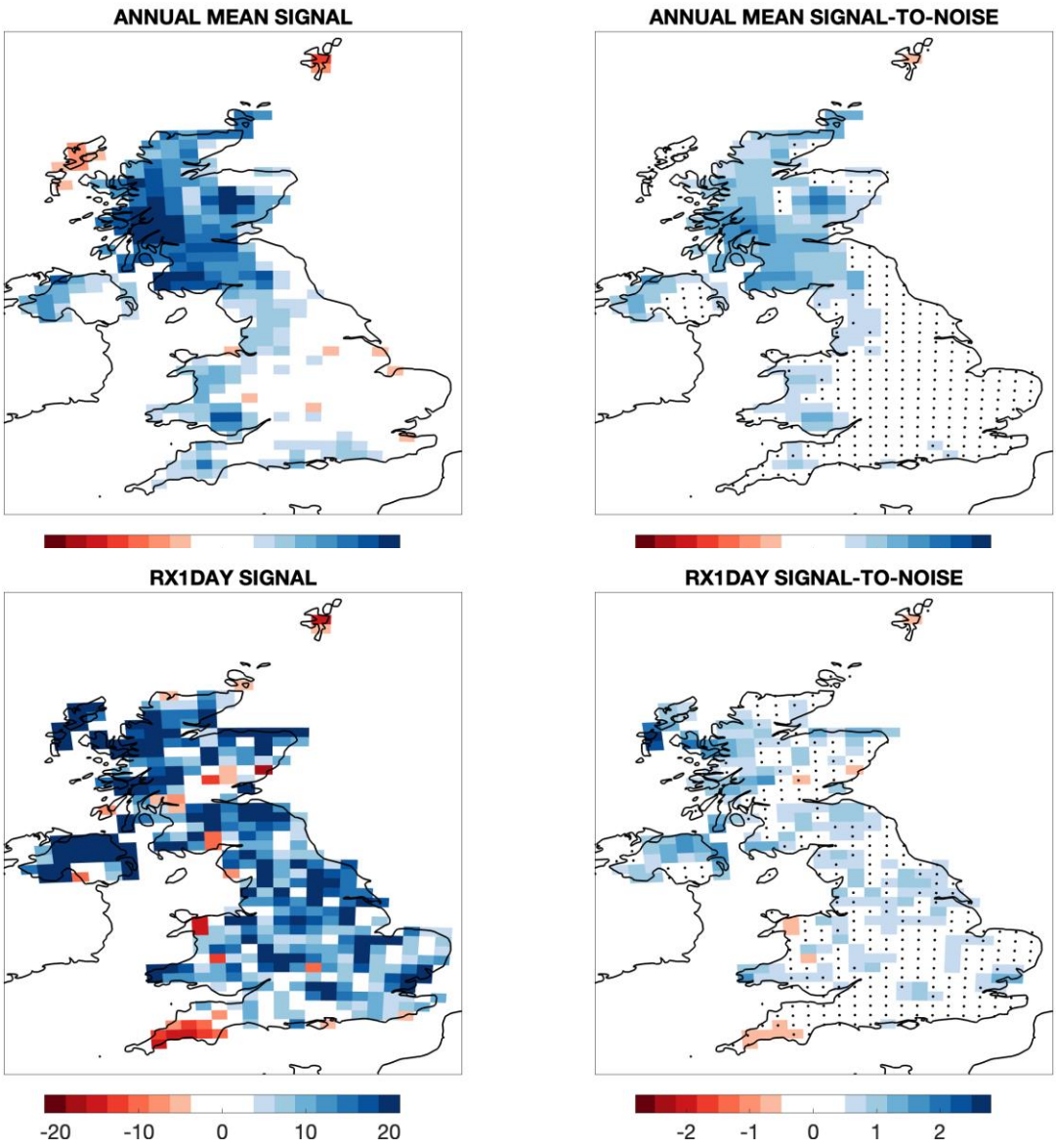

Figure 5: Signal (left) and signal-to-noise ratio (right) for annual mean precipitation over the UK (top row, 1862-2017) and extreme daily rainfall (RX1day, bottom row, 1891-2017) using the HadUK-Grid dataset. The signal is presented in units of % per K of GMST change. Blue colours denote regions becoming wetter, and red colours denote regions that are becoming drier. Stippling in the S/N panels indicates where the regression parameter is not statistically significant from zero.

Geophysical Research Letters

Supporting Information for

Observed emergence of the climate change signal: from the familiar to the unknown

E. Hawkins[1], D. Frame[2], L. Harrington[3], M. Joshi[4], A. King[5], M. Rojas[6], and R. Sutton[1]

[1] National Centre for Atmospheric Science, Department of Meteorology, University of Reading.

[2] New Zealand Climate Change Research Institute, Victoria University of Wellington, Wellington 6012, New Zealand.

[3]

[4] Climatic Research Unit, School of Environmental Sciences, University of East Anglia, UK

[5] School of Earth Sciences and ARC Centre of Excellence for Climate Extremes, University of Melbourne.

[6] Department of Geophysics and Centre for Climate and Resilience Research, CR2, University of Chile

Contents of this file

Text S1 to S3
Figures S1 to S9

S.1 Shifting distributions

The emergence of a signal can be visualised using shifting normal distributions (Fig. S1). *Frame et al.* (2017) described S/N>1 as a shift to an '*unfamiliar*' climate, S/N>2 as an '*unusual*' climate and S/N>3 as an '*unknown*' climate, in terms of an individual's lifetime. We add the term '*inconceivable*' for S/N>5, as the new mean climate would be experienced once every 3 million years in the old climate.

Two regional average examples are shown in Fig. S2, for tropical America and northern America, highlighting the differences in signal and noise characteristics. Even though northern America has a larger signal, the change is more apparent in tropical America.

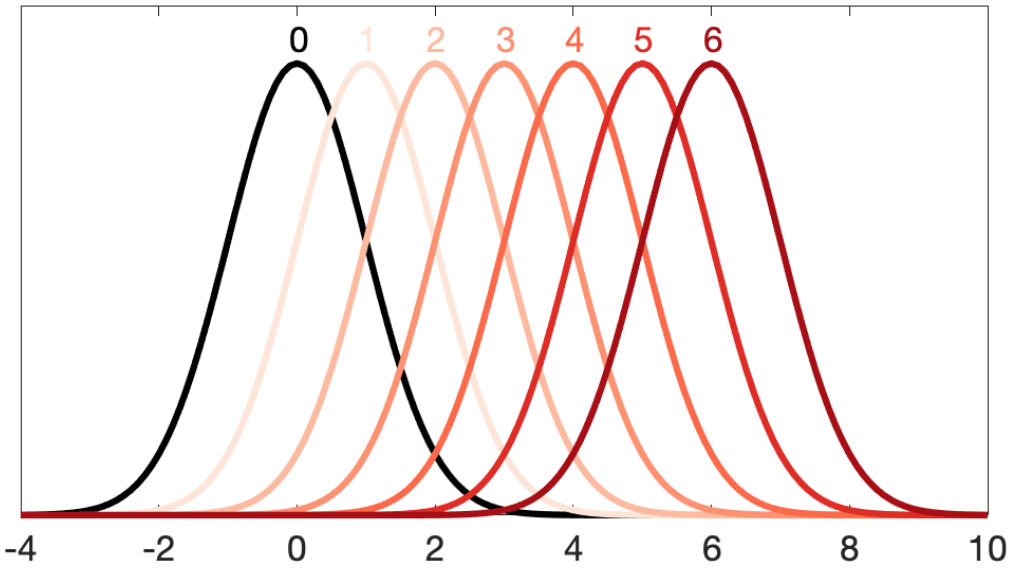

Figure S1: Shifting a normal distribution by 0 (black) to 6 (dark red) standard deviations.

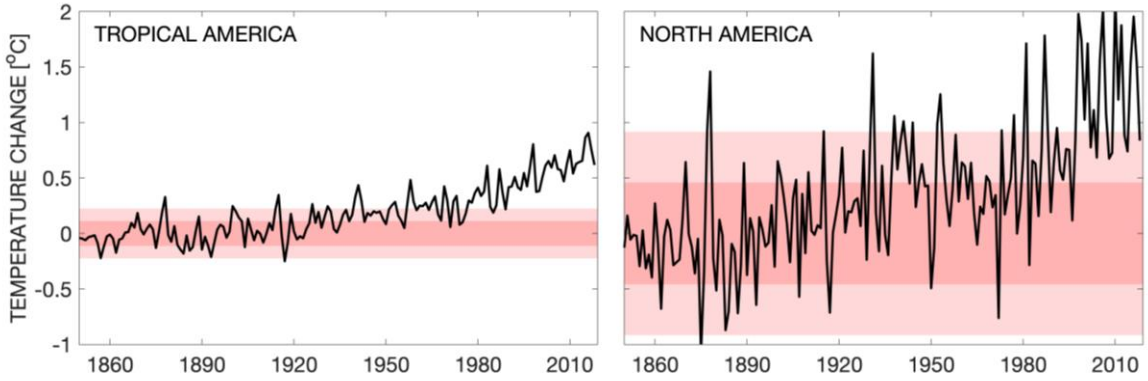

Figure S2: Two regional examples of how observed temperature changes have become apparent, using the Berkeley Earth temperature dataset. The red shaded bands represent 1 and 2 standard deviations of the noise.

S.2 Using model simulations to test the emergence methodology

We can test the robustness of the methodology to estimate the S/N using a large ensemble of model simulations. *Maher et al.* (2019) describe the 100-member ensemble of the MPI GCM, from which we use the simulated SAT for the historical period (1850-2005), extended to 2018 with the RCP4.5 scenario. First, we apply the same methodology used for the observations to each ensemble member individually. The ensemble mean S/N, which is expected to be smoother than the observed S/N due to averaging, is shown in Fig. S3a, and the spread in S/N across the ensemble is shown in Fig. S3c. The uncertainty in S/N is generally between 0.2-0.4 over land, which is typically far smaller than the mean S/N. The maritime continent, North Atlantic and Southern Ocean are regions with largest uncertainty in this GCM. The percentage uncertainty in S/N is less than 30% over most land areas (Fig. S3d). A simpler approach, which is not possible using observations, is to calculate the S/N by averaging the simulated temperature anomaly patterns in 2018, relative to the mean of 1850-1900, from all ensemble members, and dividing by the standard deviation of the 2018 anomalies (Fig. S3b). This pattern is virtually identical to Fig. S3a, highlighting that the regression approach produces S/N estimates that are robust. These results also demonstrate that the uncertainty in S/N due to simulated internal variability is relatively small.

Note that the patterns of simulated S/N in this ensemble are noticeably different from the observed patterns. One important example is in parts of west Africa where the MPI ensemble S/N is close to zero but is larger than 5 in the observations. India also has a low S/N in the ensemble, but significant values in the observations. This finding highlights the benefit of using the observations alone, as in the current study.

Fig. S4 shows the same maps for simulated precipitation change in the MPI ensemble. Again, the two methods produce similar patterns (Fig. S4a, b), with the ensemble method showing slightly larger values. The simulated uncertainty in S/N due to internal variability is typically 0.3-0.4 over land regions. The patterns are again different from that derived from the observations, especially in west Africa which is significantly wetter in the simulations but drier in the observations.

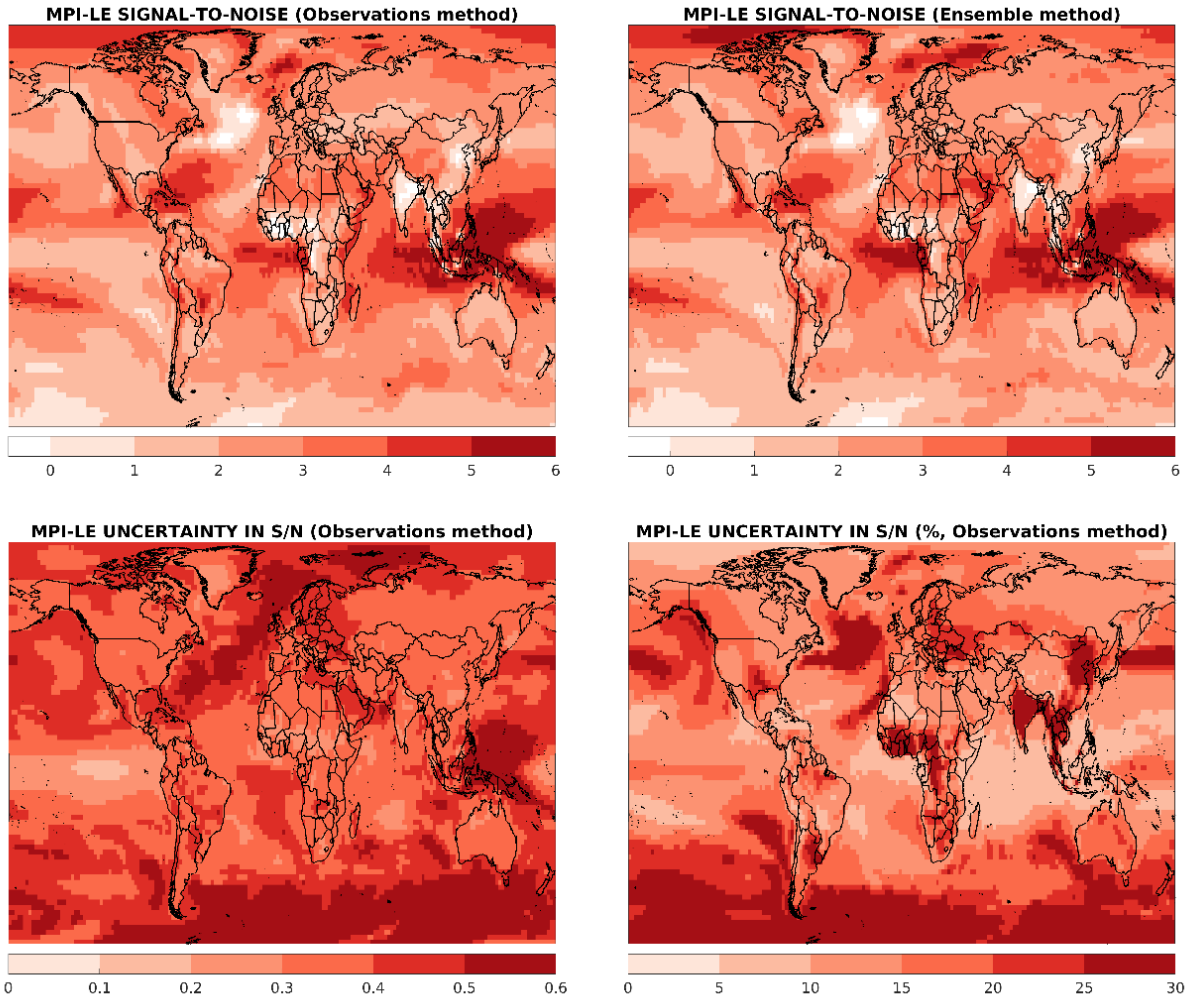

Figure S3: Testing the S/N methodology using the MPI Large Ensemble (*Maher et al.* 2019). (top left) S/N calculated as for the observations in each individual ensemble member, averaged across the 100-members. (top right) Mean simulated temperature in 2018 minus the average of 1850-1900 across all ensemble members, divided by the standard deviation of simulated temperature in 2018. (bottom left) Standard deviation in the S/N estimated using the observational method across the 100-members. (bottom right) The percentage uncertainty in S/N, i.e. bottom left panel divided by top left.

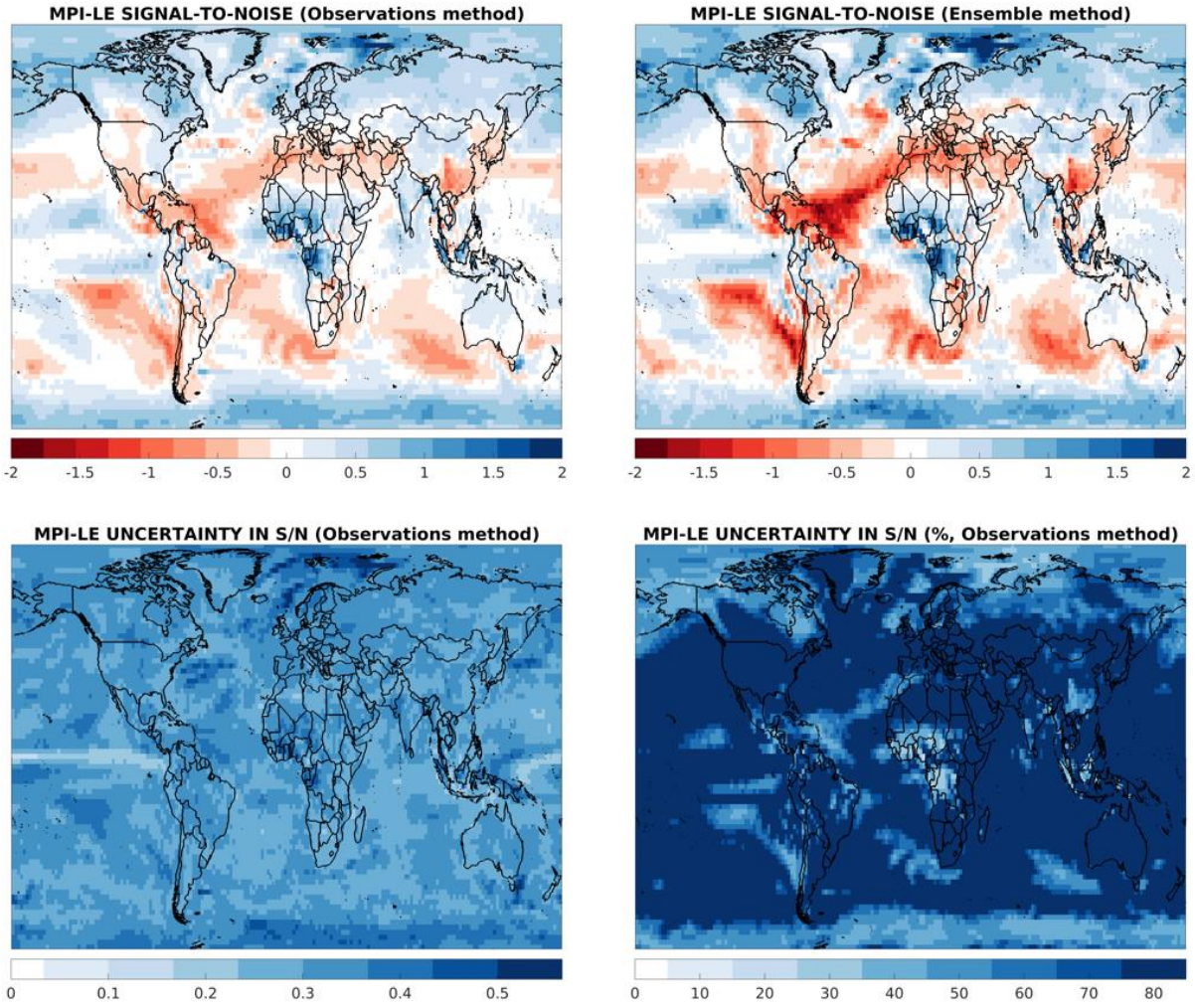

Figure S4: as Fig. S3 for precipitation**.**

S.3 Additional metrics

Figure S5 shows the fraction of land area which has a S/N for temperature exceeding the value indicated, using the Berkeley Earth dataset. For the annual mean, around 15% of the land area has a S/N larger than 5, and 40% shows a S/N larger than 2 for the warmest climatological month of the year. The warmest months tend to show larger S/N values than the coldest months.

Figure S6 repeats the S/N temperature analysis using other datasets: HadCRUT4 (*Morice et al.* 2012), *Cowtan & Way* (2014, hereafter CW14) infilled version of HadCRUT4, GISTEMP (*Lenssen et al.* 2019) and NOAA GlobTemp (*Zhang et al.* 2019). For this sensitivity test we have used the same smoothed GMST from Berkeley Earth in all cases. These datasets generally produce similar patterns to that from Berkeley Earth (Fig. 2c), but with varying amplitudes. NOAA GlobTemp has larger S/N values in the tropics than the other datasets and Berkeley Earth has larger S/N for the south-east USA. There are other notable differences for west Africa and parts of south America, mainly due to different estimates for the signal, rather than the noise (not shown). There is consistent agreement that the tropical Atlantic and Indian Oceans exhibit the highest S/N for the ocean areas, and that there has been very little warming overall in the central North Atlantic.

Figure S7 shows the S/N patterns for precipitation in different seasons, highlighting that the west Africa signals are present in all seasons except DJF, and the south-west Australia drying signal is mainly present in JJA. The wetter northern latitude signal is mainly present in DJF and MAM.

Figure S8 shows the S/N patterns for UK mean precipitation in different seasons. There are tendencies towards wetter seasons, except for JJA where the S/N is rarely significant. Note that the observed signal in southern UK is for drier summers but it has not yet emerged.

Figure S9 shows the UK mean RX1day time-series with maps for two example years.

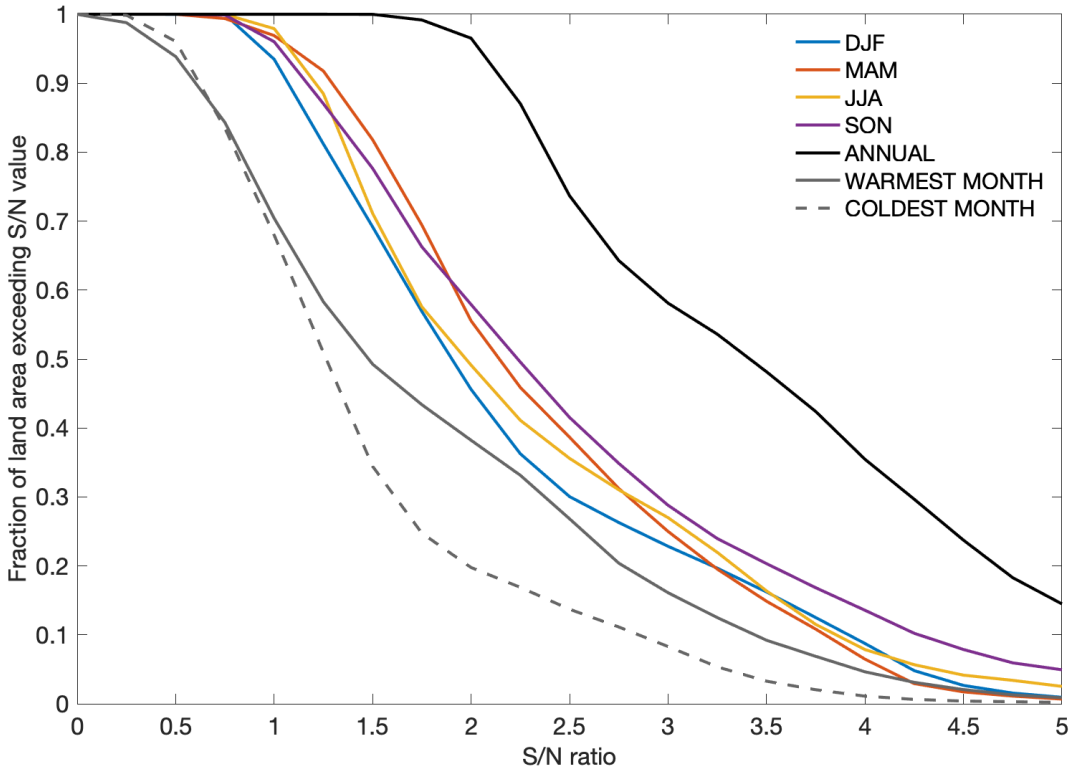

Figure S5: The fraction of land area with an observed temperature S/N larger than the ratio shown, for different seasons, the annual average, and warmest and coldest months (using the Berkeley Earth dataset).

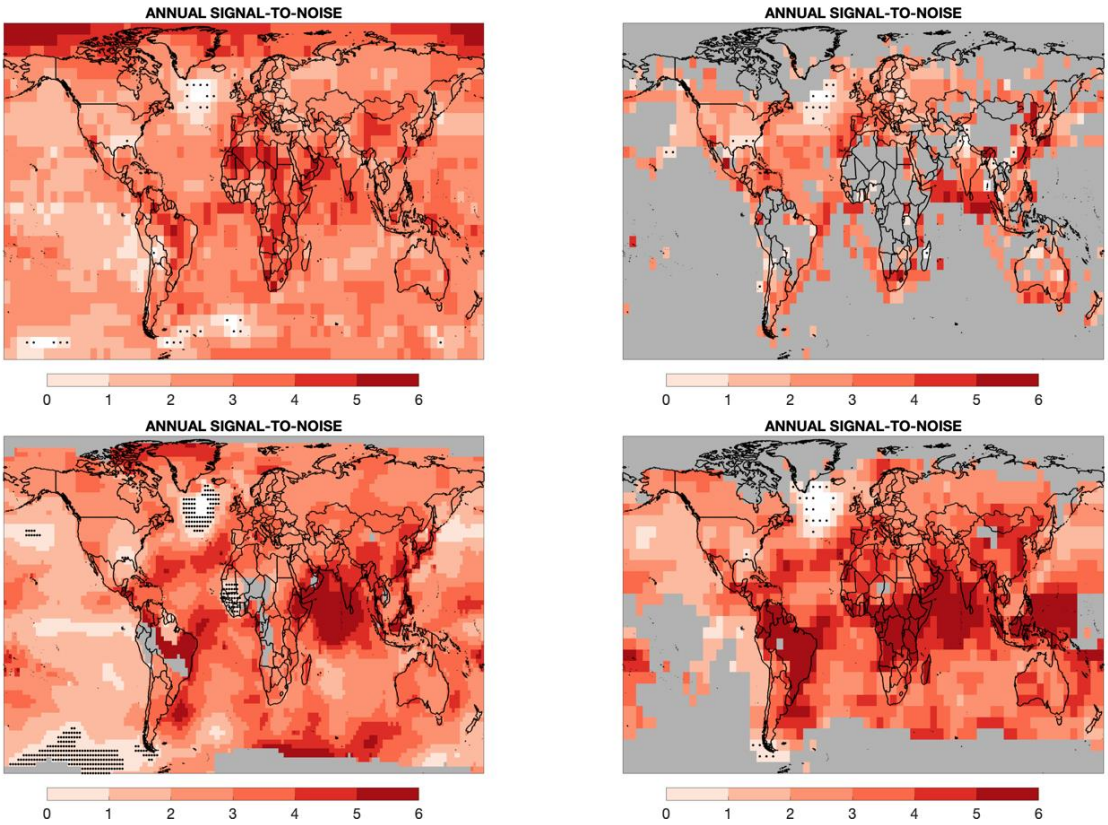

Figure S6: Observed S/N for temperature using the CW14 dataset (top left), HadCRUT4 (top right), GISTEMP (bottom left) and NOAA GlobTemp (bottom right). Stippled cells indicate that the regression coefficient is not statistically significant. Grey regions are where there is less than 100 years of data in that location for that dataset.

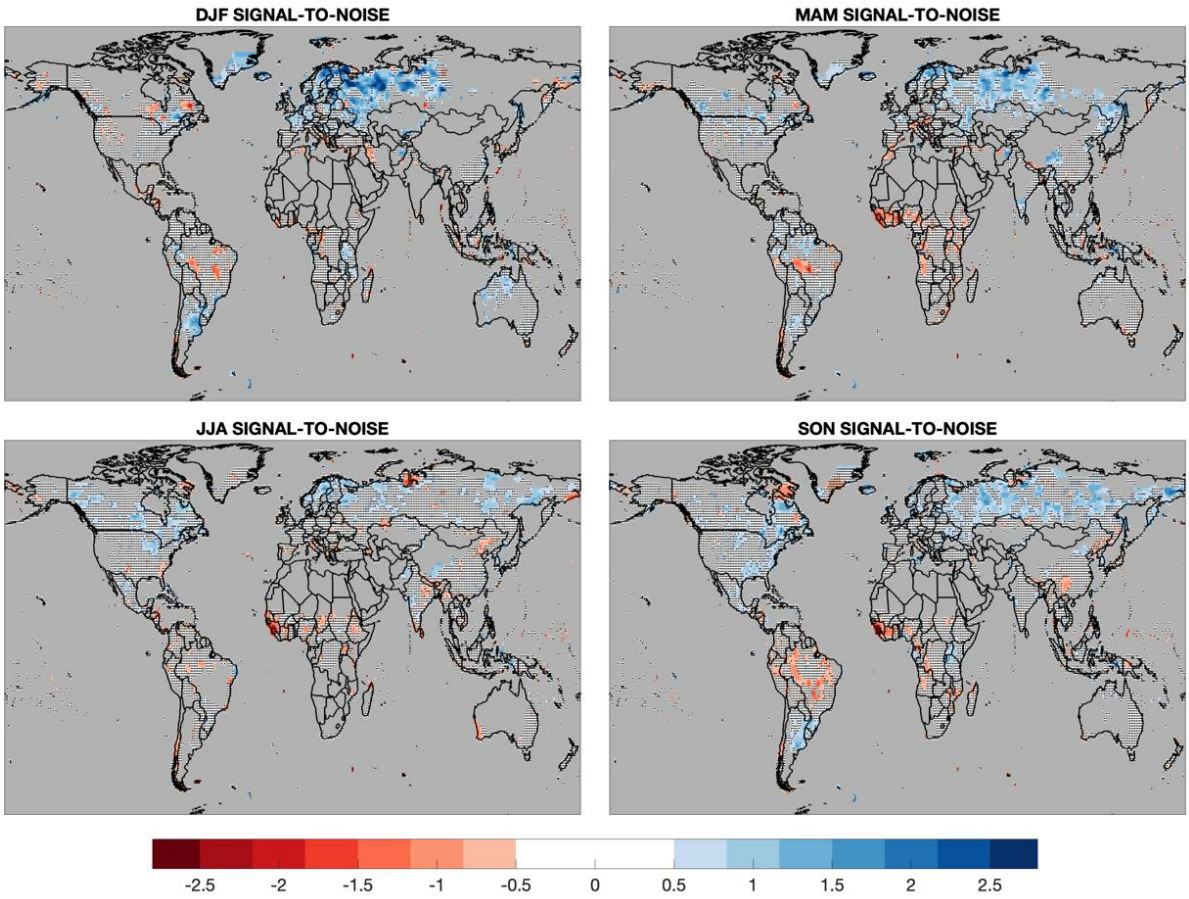

Figure S7: Signal-to-noise for precipitation in different seasons. Grey regions are either unobserved (oceans), have a seasonal precipitation of less than 62.5mm or annual precipitation less than 250mm. Stippled regions denote areas where the regression parameter is not statistically significant.

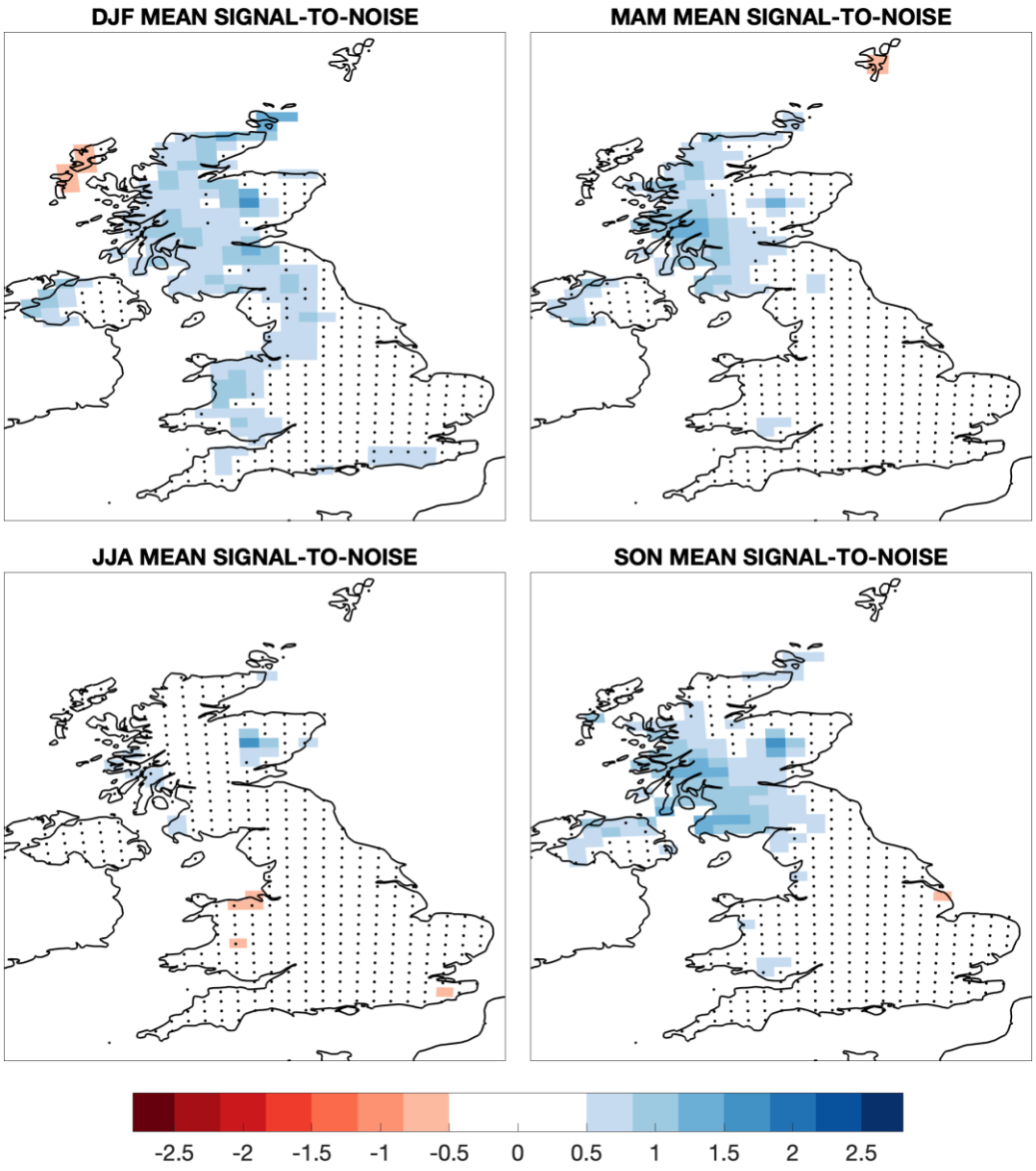

Figure S8: Signal-to-noise for UK mean precipitation in different seasons. Stippled regions denote areas where the regression parameter is not statistically significant.

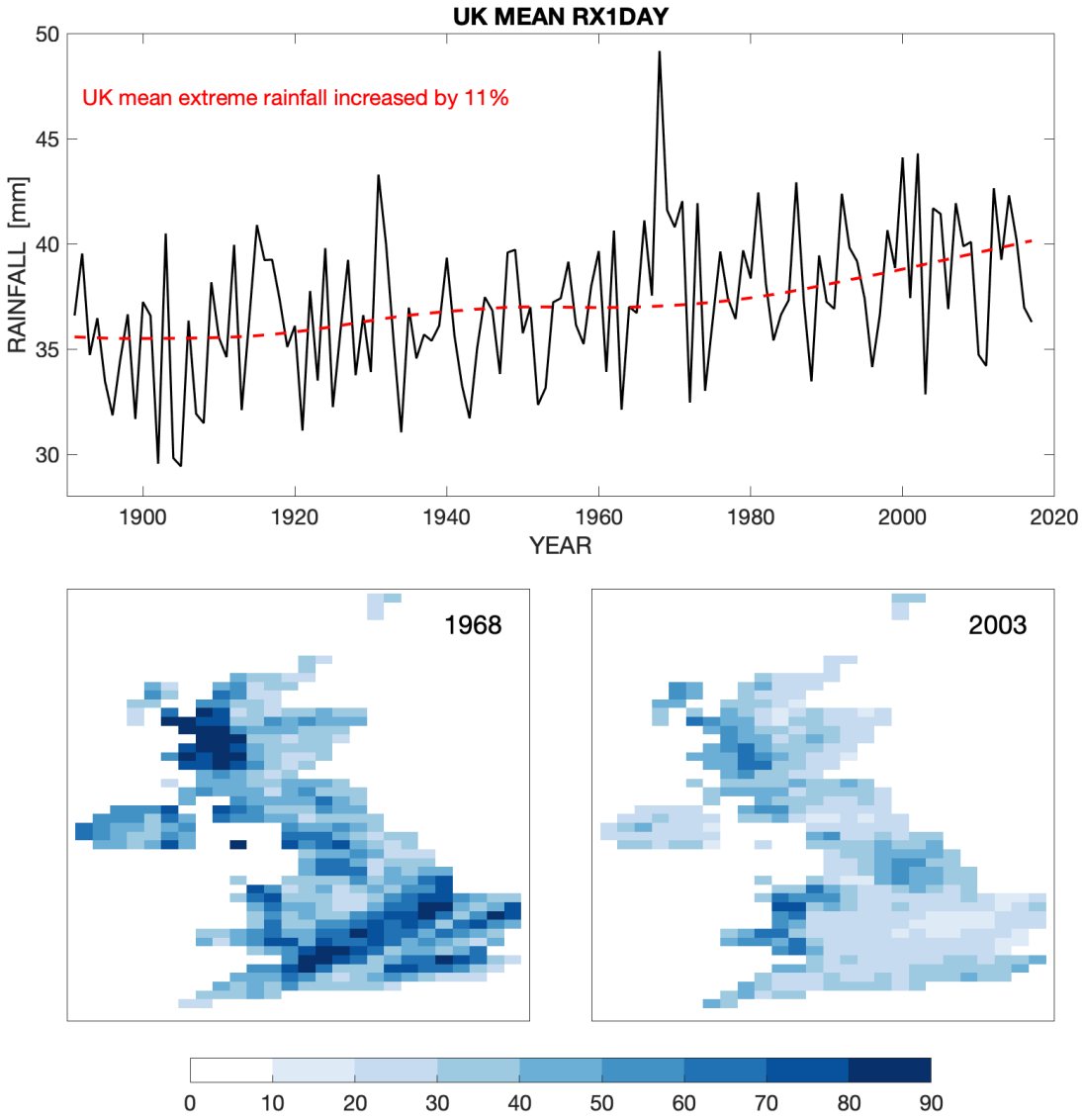

Figure S9: UK extreme rainfall (RX1day, mm): average across the UK (1891-2017, black line) and regression on GMST (red dashed line), and maps for two example years (1968 and 2003). 1968 shows the effect of three significant storm events, in contrast to 2003 which mainly shows larger rainfall over higher orographic features.